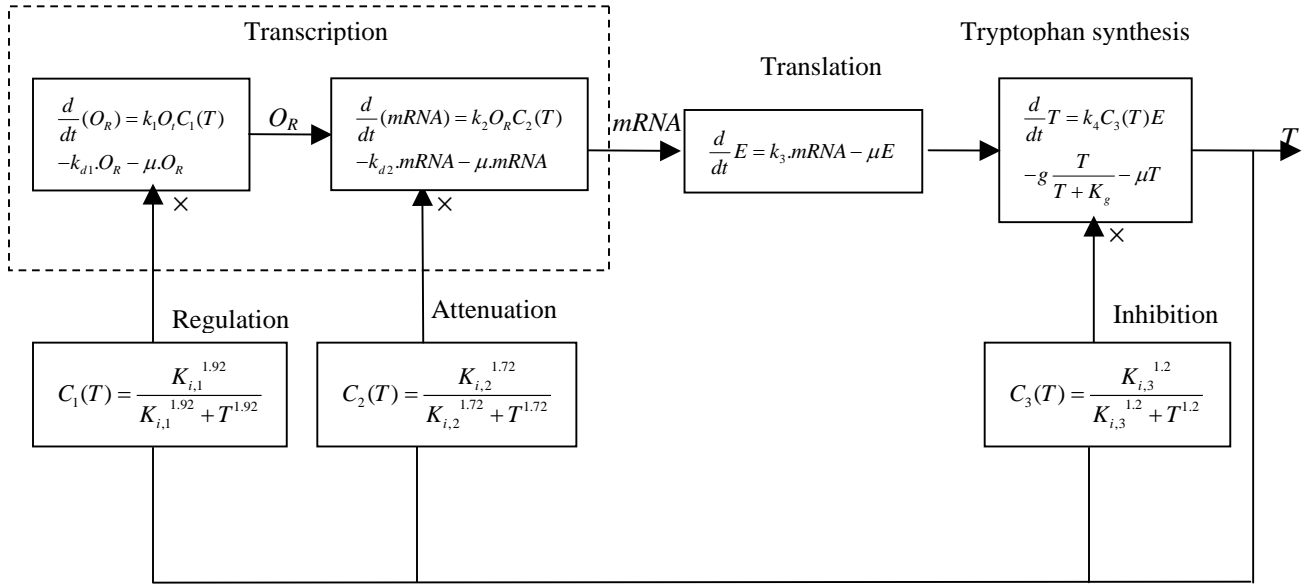
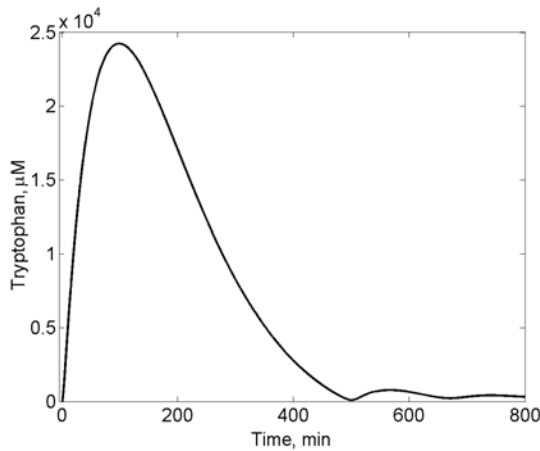


## Supplementary Material



**Fig. S1:** Block diagram of the model used for simulation of the distributed feedback structure in the *trp* system. Tryptophan concentration ( $T$ ) is independently distributed to the three-processes-in-series structure. In a conventional feedback structure, typically used in engineering systems, tryptophan concentration would have been used for genetic regulation alone (that is, controllers  $C_2(T)$  and  $C_3(T)$  would be absent).  $k_1$ ,  $k_2$ ,  $k_3$ , and  $k_4$  represent kinetic rate constants for synthesis of free operator, mRNA transcription, translation and tryptophan synthesis, respectively.  $K_{i,1}$ ,  $K_{i,2}$ , and  $K_{i,3}$  represent the half saturation constants of repression, attenuation, and inhibition, respectively.  $O_i$ ,  $\mu$ ,  $k_{d1}$  and  $k_{d2}$  refer to total operator site concentration, specific growth rate of *E. coli*, degradation of  $O_R$ , and mRNA degradation constant respectively.  $E$  represents the enzyme concentration.  $K_g$  and  $g$  are the half saturation constant and kinetic constant for the uptake of tryptophan for protein synthesis in the cell. Model parameter values are as follows (Santillan and Mackey, 2001; Bhartiya et al., 2003):  $k_1 = 50 \text{ min}^{-1}$ ;  $k_2 = 15 \text{ min}^{-1}$ ;  $k_3 = 90 \text{ min}^{-1}$ ;  $k_4 = 59 \text{ min}^{-1}$ ;  $O_i = 3.32 \text{ nM}$ ;  $k_{d1} = 0.5 \text{ min}^{-1}$ ;  $k_{d2} = 15 \text{ min}^{-1}$ ;  $\mu = 0.01 \text{ min}^{-1}$ ;  $g = 25 \text{ } \mu\text{M} \cdot \text{min}^{-1}$ ;  $K_g = 0.2 \text{ } \mu\text{M}$ ;  $K_{i,1} = 3.53 \text{ } \mu\text{M}$ ;  $K_{i,2} = 0.04 \text{ } \mu\text{M}$ ;  $K_{i,3} = 810 \text{ } \mu\text{M}$ .



**Fig. S2:** The absence of attenuation and inhibition results in a large overshoot in the tryptophan concentration (4 to 5 orders of magnitudes higher than the steady state value). Tryptophan concentration for a severely detuned  $C_1$  regulator for the mutated system is shown as the dashed curve in Fig 3b.

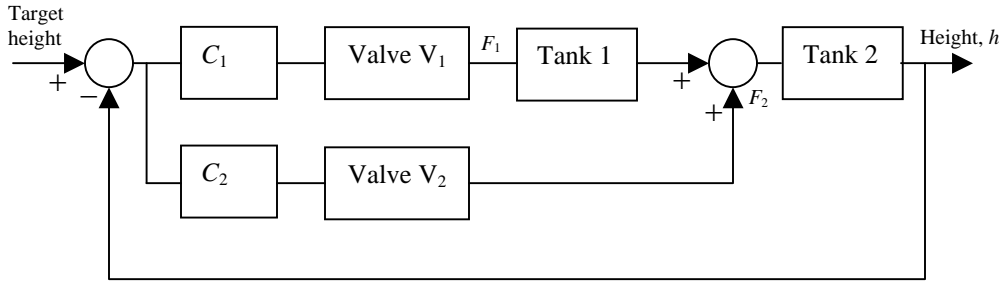


**Fig. S3:** Block diagram of the experimental two-tanks-in-series process. Regulators C1 and C2 represent PI controllers.

**Table S1:** Parameter values of the two-tank experimental setup

Nominal flow ( $F_1$ )	2.35 lpm
Area of cylindrical Tank 1 ( $A_1$ )	98.17 $cm^2$
Volume of cylindrical Tank 1	3.43 liters
Level in Tank 1 at nominal flow ( $h_{1s}$ )	17.56 cms
Drain valve coefficient ( $k_1$ ) of $D_1$	0.56 lpm/ $\sqrt{cm}$
Proportional gain of PI Controller $C_1$ ( $K_{c1}$ )	0.7 (mA/mA)
Integral time of PI Controller $C_1$ ( $\tau_{i1}$ )	3.6 min

Nominal flow ( $F_2$ )	0.35 lpm
Area of cylindrical Tank 2 ( $A_2$ )	78.54 $cm^2$
Volume of cylindrical Tank 2	4.78 liters
Level in Tank 2 at nominal flow ( $h_s$ )	26.71 cms
Drain valve coefficient ( $k_2$ ) of $D_2$	0.52 lpm/ $\sqrt{cm}$
Proportional gain of PI Controller- $C_2$ ( $K_{c2}$ )	2 (mA/mA)
Integral time of PI Controller- $C_2$ ( $\tau_{i2}$ )	4.5 min

### Model for the two-tank system

An overall volume balance for each of the two tanks yields the following nonlinear dynamic model:

$$\begin{aligned} \frac{A_1 dh_1}{dt} &= F_1 - k_1 \sqrt{h_1} \\ \frac{A_2 dh}{dt} &= k_1 \sqrt{h_1} + F_2 - k_2 \sqrt{h} \end{aligned} \quad (S-1)$$

Linearization of the above equations around a steady-state nominal point ( $h_{1s}, h_s, F_{1s}, F_{2s}$ ) followed by a Laplace transformation yields:

$$\bar{h}(s) = g_2(s) \left[ g_1(s) \bar{F}_1(s) + \frac{g_2(s)}{A_2} \bar{F}_2(s) \right] \quad (S-2)$$

where  $\bar{F}_1$  and  $\bar{F}_2$  represent the deviation from respective nominal values of the two flow rates and  $\bar{h}$  represents the deviation of the water level in Tank-2 from its nominal value. Transfer functions  $g_1(s)$  and  $g_2(s)$  represent dynamics of Tank 1 and Tank 2, respectively,

$$g_1(s) = \frac{\frac{k_1}{2A_1A_2\sqrt{h_{1s}}}}{s + \frac{k_1}{2A_1\sqrt{h_{1s}}}} \quad (\text{S-3})$$

$$g_2(s) = \frac{1}{s + \frac{k_2}{2A_2\sqrt{h_s}}} \quad (\text{S-4})$$

### Closed loop Transfer functions

The transfer function representing the dynamic relationship between the desired target and the closed loop system output is the complementary sensitivity function given as follows,

$$\bar{h}(s) = \left[ (I + L)^{-1} L \right] \bar{r}(s) \quad (\text{S-5})$$

where  $L$  represents the loop transfer function. Similarly, the closed loop transfer function from the output disturbances to the closed loop system output is denoted as the sensitivity transfer function  $S(s)$  and defined as follows,

$$S(s) = (I + L)^{-1} \quad (\text{S-6})$$

Assuming that controllers  $C_1$  and  $C_2$  are proportional controllers with gains  $K_{c1}$  and  $K_{c2}$ , the loop transfer function may be written as,

$$L = g_2(s) \left( K_{c1}g_1(s) + \frac{K_{c2}}{A_2} \right) \quad (\text{S-7})$$

### Pole-Zero Locations of the closed loop transfer function

The zeros of the closed loop system using the multiple feedback loop design denote the roots of the numerator of the closed loop transfer function Equation S-5. Similarly, the poles represent roots of the denominator of the closed loop transfer function. The pole and zero locations for the nominally designed closed loop system ( $K_{c1} = 0.7$ ;  $K_{c2} = 2$ ) are shown in Table S2.

**Table S2:** Poles and zeros for the single and multiple feedback designs in case of two-tank system. The system parameters are documented in Table S1.

Configuration	Controller Gain	Pole Location	Zero Location
Single Loop	$K_{c1} = 0.7$ $K_{c2} = 0$	$-0.66 \pm j0.075$	----
Multiple Loop	$K_{c1} = 0.7$ $K_{c2} = 2$	$-0.67 \pm j 0.078$	$-0.92$

Increasing the value of  $K_{c2}$  results in the closed loop zero approaching one of the poles. At very large values of  $K_{c2}$ , it can be shown that the system zero is located at,

$$z_1 = -\frac{k_1}{2A_1\sqrt{h_{1s}}} \quad (\text{S-8})$$

while the two poles are situated at,

$$p_1 = -\frac{k_1}{2A_1\sqrt{h_{1s}}} \text{ and } p_2 = -(1 + K_{c2}/A_2) \frac{k_2}{2A_2\sqrt{h_s}} \quad (\text{S-9})$$

resulting in cancellation of the pole corresponding to the dynamics of Tank 1 with the system zero while the other pole tends towards a large negative value indicating an increasing margin of stability.

The pole-zero movement for the single and multiple feedback designs for various values of  $K_{c1}$  and  $K_{c2}$  is shown in Fig. S4.

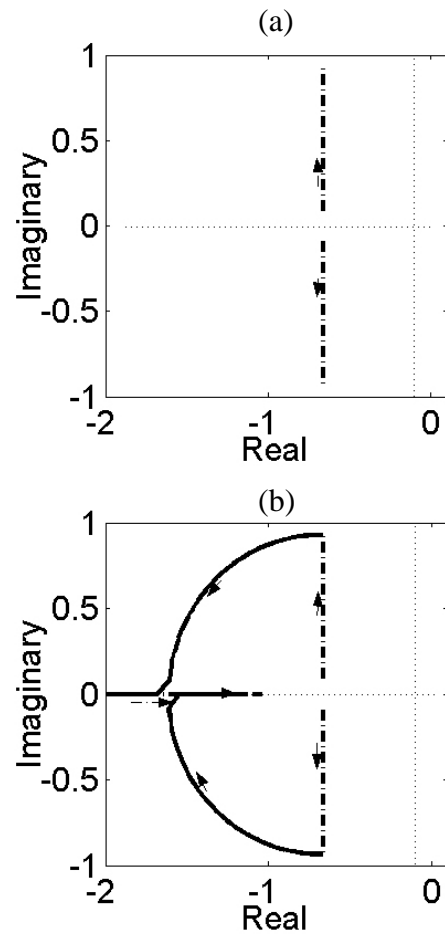


Figure S4: Root loci for a two-tanks-in-series process. (a) *Single feedback loop design* ( $K_{c2} = 0$ ): The dash-dotted line indicates the movement of the two poles with increasing values of  $K_{c1}$ . The two poles move parallel to the imaginary axis and away from the real axis. No system zeros exist in this design. (b) *Multiple feedback loop design*: The dash-dotted line indicate the movement of the poles when  $K_{c2} = 0$  (single feedback loop design). The solid line represents the movement of the pole when  $K_{c2}$  increases from its zero value resulting in the two poles moving towards the real axis. The system zero moves along the real axis and is indicated by the horizontal dash-dotted line. For large values of  $K_{c2}$ , one of the two poles and the zero are in close proximity and represent a pole-zero cancellation.

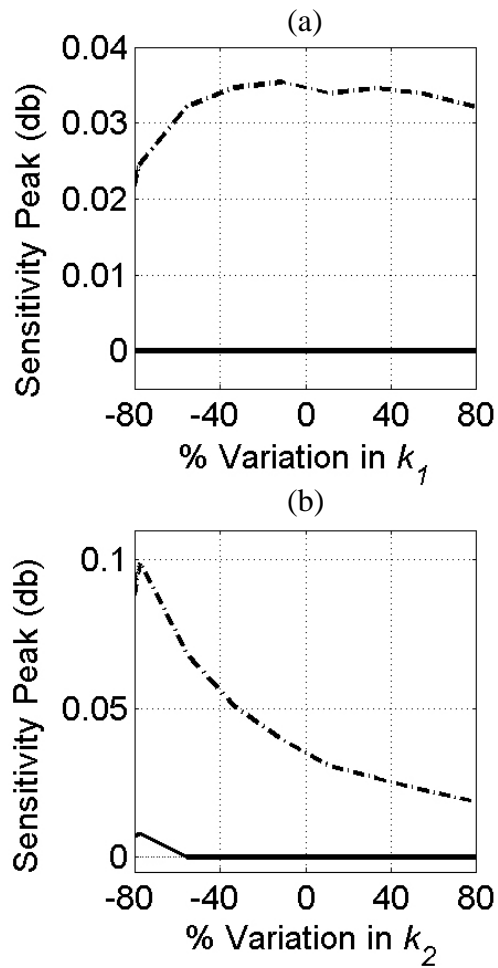


Figure S5: Variation of the peak value of the sensitivity transfer function with process parameters using the single feedback (dash-dotted) and multiple feedback (solid) designs. (a) Variation in the valve coefficient  $k_1$  of drain valve  $D_1$ , (b) Variation in the valve coefficient  $k_2$  of drain valve  $D_2$ .